Published in final edited form as:

Cancer Res. 2016 November 01; 76(21): 6230–6240. doi:10.1158/0008-5472.CAN-16-0618.

CCL22 DIVERTS T REGULATORY CELLS AND CONTROLS THE GROWTH OF MELANOMA

Jared Klarquist[1], **Kristen Tobin**[2], **Peyman Farhangi Oskuei**[1], **Steven W. Henning**[1], **Manuel F. Fernandez**[1], **Emilia R. Dellacecca**[1], **Flor C. Navarro**[1], **Jonathan M. Eby**[1], **Shilpak Chatterjee**[3], **Shikhar Mehrotra**[3], **Joseph I. Clark**[1,2], and **I. Caroline Le Poole**[1,4]

[1]Oncology Research Institute, Loyola University Chicago, Maywood (IL)

[2]Department of Medicine, Loyola University Chicago, Maywood (IL)

[3]Department of Surgery/ Hollings Cancer Center, Medical University of South Carolina, Charleston (SC)

[4]Departments of Pathology, Microbiology and Immunology, Loyola University Chicago, Maywood (IL).

Abstract

T regulatory cells (Treg) avert autoimmunity but their increased levels in melanoma confer a poor prognosis. To explore the basis for Treg accumulation in melanoma, we evaluated chemokine expression in patients. A 5-fold increase was documented in the Treg chemoattractants CCL22 and CCL1 in melanoma-affected skin versus unaffected skin, as accompanied by infiltrating FoxP3+ T cells. In parallel, there was a ~2-fold enhancement in expression of CCR4 in circulating Treg but not T effector cells. We hypothesized that redirecting Treg away from tumors might suppress autoimmune side-effects caused by immune checkpoint therapeutics now used widely in the clinic. In assessing this hypothesis, we observed a marked increase in skin Treg in mice vaccinated with CCL22, with repetitive vaccination sufficient to limit Treg accumulation and melanoma growth in the lungs of animals challenged by tumor cell injection, whether using a prevention or treatment protocol design. The observed change in Treg accumulation in this setting could not be explained by Treg conversion. Overall, our findings offered a preclinical proof of concept for the potential use of CCL22 delivered by local injection as a strategy to enhance the efficacious response to immune checkpoint therapy while suppressing its autoimmune side-effects.

Keywords

CCL22; Treg; trafficking; melanoma; autoimmune

Correspondence I. Caroline Le Poole Ph.D., Professor of Pathology, Microbiology and Immunology, Tumor Immunology and Immunotherapy Research Program, Loyola University Chicago, Cardinal Bernardin Cancer Center Rm 203, 2160 South 1st Avenue, Maywood, IL 60153, USA, ilepool@luc.edu, Tel 1-708-327-2032 (office) / 1-708-327-3138 (lab), Fax 1-708-327-3138.

The authors have no conflicts of interest to report.

INTRODUCTION

Treg suppress the function of dendritic cells (DCs), B cells and T cells in a contact-mediated fashion (1). When tumors develop, the expansion of Treg interfering with successful immune surveillance is a natural extension of this process (2). The abundance of peripherally induced Treg, correlates with enhanced tumor growth (3). New tumor types where progression is correlated with Treg infiltration continue to be identified (4), and an even greater cohort of patients will face Treg mediated immunosuppression in the future. Thus a solid understanding of intratumoral Treg accumulation is important.

An increased abundance of Treg within tumors can result from enhanced proliferation, for example when Treg recognize antigen (3). Also, the tumor can instruct infiltrating T cells to convert into Treg, for example through thioredoxin expression (2). The plasticity of Th17 may play a role, giving rise to Treg by conversion in the presence of intratumoral IL-10 (5). Another mechanism supporting Treg abundance is chemoattraction (6). Among chemokines that can attract Treg, CCL22 may be particularly important (7). Elevated expression of CCL22 is observed in diverse tumor types (8, 9). Simultaneously elevated expression of receptors for CCL22 and other chemokines helps to explain an overabundance of Treg (10). The intratumoral vasculature will likewise impact Treg extravasation and tumor infiltration (11).

To reduce Treg abundance and support anti-tumor immunotherapy, patients can be pre-treated with antibodies. In practice, this challenge has primarily been met by antibodies to the IL-2 receptor CD25, yet such treatment also depletes activated effector T cells. Limiting Treg activation through an immune checkpoint blockade can also be of help (12). Finally, depletion using antibodies to CCR4 may be useful. This concept is being explored using mogamulizumab infusion in a clinical trial (13).

Systemic depletion of Treg can be associated with autoimmunity (14). In fact, underrepresentation of Treg is common in autoimmune conditions (15). A direct link between local underrepresentation of Treg and autoimmunity can be made in tissue specific conditions, such as vitiligo (16). The abundance of Treg is reduced, apparently in response to limited numbers of CCL22-producing cells, including macrophages (17). In models of vitiligo, Treg depletion can induce depigmentation even in the absence of IFN-γ, highlighting their relative importance (18).

As tumor immunotherapeutic approaches meet with increased success, the development of autoimmunity takes center stage. This highlights the need for the development of precise Treg depletion strategies. We recently demonstrated that Treg can be drawn to the skin by local Ccl22 overexpression (19). To simultaneously address the accumulation of Treg in melanoma and their shortfall in autoimmunity, we postulate that cutaneous overexpression of CCL22 can divert Treg away from tumors and into the skin, as highlighted in Fig. 1.

Here, we describe the abundance of relevant chemokines in human melanoma by immunostaining. We also evaluated chemokine receptor expression levels in Treg from patients and controls, and compared this to expression by CTL. Looking to Ccl22-mediated chemoattraction of Treg to the skin and its success towards mitigating autoimmune

depigmentation, we applied our strategy in a mouse model of metastatic melanoma using B16 tumor cells. We measured the consequences of cutaneous Ccl22 overexpression for tumor growth and intratumoral Treg abundance, and addressed the possibility that cells may be converted to Treg on site or preferentially migrate towards Ccl22. We propose that cutaneous Ccl22 overexpression can support anti-tumor responses while suppressing autoimmune side effects of immunotherapy.

MATERIALS AND METHODS

Human and mouse subjects

Melanoma *in situ* and metastatic melanoma surgical samples not required for pathologic examination and 30 ml blood samples from metastatic melanoma patients were obtained after informed consent under IRB approved protocols according to the declaration of Helsinki. Metastatic tissue samples were obtained from spine, lung, lymph node or brain, whereas melanoma *in situ* samples were skin-derived. In concordance with the approved protocols, no further patient information was shared with investigators. Normal human skin was obtained as otherwise discarded, fresh surgical tissue and normal human buffy coats were from LifeSource (Chicago, IL). No personal identifiers were provided to investigators, and studies were approved by the Institutional Review Board. Incoming blood samples were given a tissue sample number before subjecting the samples to Ficol density gradient centrifugation to enrich the lymphocytes. Resulting PBMC were stored in our LN2 inventory by tissue number until use. Tissue samples were embedded in optimal cutting temperature (OCT) compound (Sakura Finetek, Torrence, CA), snap frozen in liquid nitrogen and stored at −80°C. Eight μm frozen sections were cut, fixed in acetone at 4°C and stored at −20°C until use. For mouse experiments approved by the Loyola IACUC, 6 week old C57BL/6, Pmel-1 (gp100 reactive, TCR transgenic mice) and Foxp3-eGFP (Treg reporter) mice were purchased from Jackson Laboratories (Bar Harbor, ME) under IACUC approval at Loyola University Chicago and bred in house. Skin and pulmonary tissues were harvested at euthanasia and stored at −80 °C.

Immunostaining of human and mouse tissues

Eight μm human tissue cryosections were preincubated with 10% normal human AB serum (Gemini Bio-Products, Calabasas, CA). When staining mouse tissues, sections were fixed in 10% SP-buffered formalin. Sections were subsequently treated with SuperBlock (ScyTek Laboratories, West Logan, UT) and with 0.3% H_2O_2 to inactivate endogenous peroxidase. When detecting nuclear FoxP3 in mouse tissues, antigen retrieval was pursued after incubation with the primary antibody by using a sequence of 0.05% Tween (Sigma Life Sciences, St. Louis, MO), 1% Triton-X100 (Fischer Scientific, Hampton, NH) and 0.05% Tween, each in TBS. Primary antibodies include clones Ta99 to TRP-1 (Covance, Madison, WI), polyclonal rabbit antiserum to mouse and human FoxP3 (ThermoFisher, Rockford, IL) or MF-14^{PE} rat monoclonal to mouse FoxP3 (Biolegend, San Diego, CA), 145-2C11$^{bio,\ FITC\ or\ PE}$ to mouse CD3ε (BD Biosciences, Franklin Lakes, NJ) or HIT3A^{FITC} to human CD3 (BD Biosciences), PK138$^{Alexa\ Fluor\ 488}$ to mouse NK1.1 (BioLegend, San Diego, CA), 8P16-N4-L21 to human CCL1 (Enzo Life Sciences, Farmingdale, NY), 57203 to human CCL22 (R&D Systems, Minneapolis, MN) and

MAB4391 to mouse Ccl22 (R&D Systems), TG6/CCR4 to human CCR4 (BioLegend, San Diego, CA) and 191704 to human CCR8 (R&D Systems). For immunofluorescent stainings, slides were coverslipped with anti-fade reagent with DAPI (Life Technologies, Fischer Scientific, Hampton, NH). For immunoenzymatic stains, primary antibodies were detected using biotinylated rabbit anti-mouse Ig (Dakopatts, Glostrup, Denmark) combined with horseradish peroxidase-labeled streptavidin (Dakopatts) or goat anti-rabbit Ig (Dakopatts). For TUNEL stainings an Apoptag kit (Millipore, Darmstadt, Germany) was used. Unfixed tissues were incubated with Ta99 Ab to TRP-1 prior to formalin fixation and incubation with TDT enzyme. Alkaline phosphatase labeled polyclonal goat anti-mouse IgG (Dakopatts, Glostrup, Denmark) was combined with peroxidase-labeled anti-dioxigenin. Alkaline phosphatase was detected using detected with FAST Blue BB substrate (Sigma-Aldrich, St. Louis, MO). Aminoethylcarbazole (AEC) was used as a peroxidase substrate (Sigma-Aldrich). Some slides were counterstained in Harris hematoxylin (Sigma Aldrich) before coverslipping in glycergel (Dakopatts). Stainings were imaged using an Olympus Scope BX53 (Center Valley, PA) with a Retiga 4000R 4.2 Mpixel monochrome camera (QImaging, Surrey (BC), Canada), followed by Adobe Photoshop-supported (Adobe Systems Incorporated, San Jose, CA) quantification of stained cells. In skin tissues stained cells were analyzed within a dermal area to a depth of 3x epidermal height without reference to tumor location.

Treg conversion and migration analysis

To measure conversion of T cells into Treg *in vitro*, we exposed mouse splenocytes from a FoxP3-eGFP reporter mouse to cytokines. Briefly, 10^6 splenocytes were incubated in 24 well plates (Corning Inc. Life Sciences, Lowell, MA, USA), in X-VIVO 20 media (Cambrex, Walkersville, MD, USA) in presence of mCcl22 (5, 50 or 500 ng/mL), human TGF-β (0.2, 2 or 20 ng/mL) or media alone in triplicate wells. After 18 hrs, samples were individually analyzed for expression of CD3, CD25 and FoxP3 expression by FACS to identify Treg. The percentage of $CD25^+$, $FoxP3^+$ Treg among $CD3^+$ T cells was graphed. For transwell migration assays, 10^6 splenocytes from FoxP3-eGFP mice were added in triplicate to a 5μm pore size transwell insert (Costar, New York, NY) with the outer well containing chemokines Ccl1 or Ccl22 (R&D Sytems, Minneapolis, MA) at the indicated concentrations. The Treg fraction was measured as reporter gene expressing cells among total cells by FACS analysis of the top and bottom wells after 2 hrs.

Fluorocytometry of human PBMC

Approximately 3 million PBMC were thawed for negative magnetic T cell sorting using a labeled $CD3^+$ enrichment antibody cocktail (StemCell Technologies, Vancouver, BC). Monoclonal antibodies used for FACS analysis and sorting of peripheral blood samples include antibodies to human CD3 (clone F7.2.38, BD Biosciences, San Jose, CA); $CD4^{FITC}$ (clone RPA-T4, BD Biosciences); $FoxP3^{PE}$ (clone 206D, Biolegend, San Diego, CA); $CD25^{PE\text{-}Cy7}$ (clone M-A251, BD Biosciences) or $CD25^{PE}$ (clone 4E3, MACS Miltenyi Biotech, Auburn, CA); $CD127^{APC\text{-}eFlour780}$ (clone eBioRDR5, eBioscience, San Diego, CA); $CCR4^{PerCP\text{-}Cy5.5}$ (clone TG6/CCR4, Biolegend); $CCR8^{APC}$ (clone FAB1429A, R&D Systems, Minneapolis, MN); CLA^{bio} ($HECA452^{bio}$) with $streptavidin^{Pacific\ Orange}$ (Invitrogen, Carlsbad, CA). T lymphocytes were then first incubated in presence of

antibodies CLA^{bio}, CCR4$^{PerCP\text{-}Cy5.5}$ and CCR8^{APC}, subsequently adding CD4^{FITC}, CD25 $^{PE\text{-}Cy7}$ and CD127$^{APC\text{-}eFlour780}$ to distinguish Tregs. Washed cells were incubated with streptavidin$^{Pacific\ Orange}$, followed by permeabilization and intracellular staining with anti-FoxP3^{PE} according to the manufacturers' protocol (BioLegend, San Diego, CA). For gating purposes an FMO (FoxP3 excluded), and a fluorescence minus three control (CCR4, CCR8 and CLA excluded) were used. Multicolor analysis of >200,000 acquired events was performed using the FACSCanto II (BD Biosciences) and Flowjo analysis software (TreeStar, Cupertino, CA). A population enriched for CD8+ effector T cells was selected as CD4^{-} T cells among presorted T cells.

Gene gun vaccination

Ccl22 DNA or empty vector coated microparticles were introduced into mouse skin using a Helios Gene gun (Bio-Rad, Hercules, CA). One μm gold microparticles (Alfa Aesar, Ward Hill, MA) were coated with mouse Ccl22-encoding cDNA expressed under a CMV promoter in pcDNA3.1 (19). DNA was precipitated onto gold particles in presence of spermidine (Sigma-Aldrich) and used to coat Tefzel tubing (Bio-Rad). Mice were Naired (Church & Dwight, Ewing, NJ) prior to vaccination under isoflurane anesthesia (E-Z Systems, Paler, PA) with 4.8 μg DNA. Mice were vaccinated before tumor challenge every 6 days, or after tumor challenge every 5 days. Prior findings indicated that continued treatment was necessary to maintain elevated levels of cutaneous Treg (19).

Measuring tumor growth

In prophylactic experiments, mice were challenged with 10^5 B16F10 mouse melanoma cells by retro-orbital injection after 6 vaccinations at 6 day intervals. In therapeutic experiments, vaccinations were performed at 5 day intervals starting 3 days after tumor challenge. CRL-6475 mouse melanoma cells were obtained from the ATCC (Manassas, VA) providing standardized authentication and quality testing, expanded in Dulbecco's Modified Eagle's Medium with 10% fetal bovine serum and antibiotic/antimycotic (all from Thermo Fisher Scientific, Waltham, MA) and passaged twice before storing stock vials in LN2 upon confluence within 3 weeks of purchase. A stock vial was thawed and plated 16 months later and passaged once before being harvested for tumor injections. Another aliquot plated two weeks later tested pathogen-free by Charles River Laboratories (Wilmington, MA) using a rodent agent 360° PCR panel. B16 cells consistently showed >95% viability upon thaw. Tumor challenged mice received continued vaccinations with Ccl22 or empty vector DNA for 9 days (prophylactic experiments) or 18 days (therapeutic experiments) before euthanasia. Lungs were imaged and surface pulmonary metastases were enumerated as melanized growths per pulmonary surface area prior to snap freezing the OCT-embedded tissues (Tissue Tek). In therapeutic experiments the % area occupied by tumor calculated in ImageJ (20) was used as the more accurate estimate of tumor burden. Tissues were immunostained to confirm metastatic invasion and to detect infiltrating Treg.

Statistical comparisons

When two groups were compared as in melanoma and control lymphocytes or Ccl22 treated and empty vector treated mice, a t-test for groups of unequal variance was applied. In therapeutic experiments where tumors were followed for 18 days and larger group sizes

were included, trimmed means were used. For comparisons among multiple groups, an ANOVA was used followed by Dunnett's multiple comparison test to compare treatment samples to an untreated control group.

RESULTS

Treg chemokines are expressed within human melanoma tumors

Immunohistology provided a first impression of Treg homing in melanoma. Representative serial sections are shown in Fig. 2. Immunostaining of a metastatic tumor in Fig. 2A illustrates tumor cells tightly packed in a central tumor area. Just outside, sparsely differentiated tumor tissue displays irregular TRP-1 staining, where Treg are abundant as the same area is comprised primarily of $FoxP3^+$ cells (Fig. 2B). Treg express CCR4 (Fig. 2C) whereas CCL22 expression is at times punctate (Fig. 2D). Expression of CCR8 (Fig. 2E) and its ligand CCL1 (Fig. 2F) is found outside the central tumor area (Fig. 2D). In metastatic tumors of the lung (2G), lymph node (2H) or brain (2I) a similar distribution of CCL22 expressing cells is found (arrows). Thus, chemoattractant cytokines may support Treg homing to the tumor. We quantified CCL22 and CCL1 expressing cells in four samples of melanoma in situ and superficial spreading melanoma, compared to 4 samples of control skin; the majority of unaffected tissues (3/4) originated from metastatic melanoma patients. An impressive 5-fold increase in the expression of CCL22 (2J) and an average 45-fold increase in the number of CCL1 expressing cells ($P<0.05$) (2K) was observed in melanoma-affected skin, suggesting that Treg are preferentially attracted towards tumors.

Enhanced expression of homing markers by Treg from melanoma patients

Besides enhanced expression of chemokines, accumulation of Treg in tumors can be driven by homing marker expression on the surface of circulating Treg. We stained lymphocytes from blood samples of 5 melanoma patients and 5 healthy controls, selecting Treg based on expression of $CD4^+$, $CD25^+$, $CD127^{low}$ and $FoxP3^+$ among singlets as shown in Fig. 3A. The resulting percentages of Treg among lymphocytes were not significantly different at 2.3 +/− 0.5% among healthy controls and 3.0 +/−1% among patient samples. Expression of CCR4, CCR8 and CLA (cutaneous lymphocyte antigen) was evaluated. Both the % stained Treg (Fig. 3B) and the mean fluorescence intensity (Fig. 3C) among CCR4 expressing cells was increased among melanoma patients ($P<0.05$), with 16% more Tregs staining at a 1.9-fold increased intensity. Similarly, 1.5% more melanoma Treg expressed CCR8 at a 1.6-fold increased intensity overall. By comparison, the expression of CLA did not vary among patient and control Treg. These findings suggested that anti-tumor responses can be manipulated by interfering with Treg homing if chemokine receptor expression does not likewise increase on effector lymphocytes. We thus evaluated expression of chemokine receptors on non-CD4 T cells (primarily CTL) in Fig. 4. Interestingly, these T cells display no differences in CCR4 or in CLA expression, whereas a trend towards increased CCR8 expression was observed among CTL. When comparing $CCR8^+$ lymphocytes among melanoma patients and controls, CCR8 was expressed not only by a 2-fold greater percentage of patient Treg ($P<0.05$), but also among a 2.5-fold greater percentage of patient CTL ($P<0.05$), thus targeting CCR8 and its interaction with CCL1 would not be fortuitous (not shown). However, expression of CCR4 is much greater among Treg compared to CTL,

rendering the CCR4-CCL22 axis a valuable interaction to interfere with in melanoma. Enhanced expression of CLA on Treg compared to $CD8^+$ T cells suggests that blocking this receptor would also relatively favor CTL infiltration, however, targeting the chemokine receptor CCR4 may be a better choice based on the 3.1-fold greater % expressing melanoma Tregs in Fig. 3 ($P<0.001$). Thus, targeting the CCR4/CCL22 axis would be preferable for therapeutic applications.

Cutaneous overexpression of Ccl22 diverts Treg

Gene gun vaccination provides a mode of mechanical transfection of cutaneous cells. Marked overexpression of Ccl22 in vaccinated skin was previously demonstrated, and the same protocol was used here (19). At euthanasia, we found a trend towards a 2-fold increase in Ccl22 expressing cells in the spleen ($n=6$, $P=0.07$), yet the main site of overexpression was the skin, where the gold beads concentrated at the vaccination site. Ccl22 vaccination dramatically reduced vitiligo development in T cell receptor transgenic Pmel-1 mice, where T cells respond to gp100 (19). Here, we tested whether Ccl22 may convert skin and tumor infiltrating T cells into Treg, as reported for TGF-β. Splenocytes from FoxP3-eGFP reported mice were exposed to Ccl22, TGF-β or medium for 18 hours before quantifying Tregs by FACS analysis. As shown in Fig. 5A-C, in example FACS plots generated under each culture condition and 5D where Tregs are quantified, exposure to Ccl22 did not induce a greater Treg compartment among splenocytes at any tested concentration, even at higher than physiologic (serum) concentrations (21). However, comparing TGF-β treatment to untreated cells indicates a significant treatment effect by ANOVA ($P=0.0002$), and the % of Treg is significantly different from untreated samples ($P<0.05$) at both 2 and 20 ng/mL using Dunnett's multiple comparison post-test. In transwell migration assays (22) Treg were significantly enriched among total splenocytes migrating towards Ccl22 (Fig. 5E) but not towards Ccl1 (Fig. 5F). Taken together, these data sparked the concept that Treg can be diverted to the skin, providing a tumor microenvironment more conducive to tumor immune surveillance.

A strategy to contain tumor growth

An important advantage of redirecting Treg over simply blocking Treg tumor homing by antibodies to deplete Treg is that skin-migrating Treg can suppress autoimmunity. We tumor-challenged Ccl22-vaccinated mice and continued to treat the animals by gene gun vaccination until dissection (Fig. 6A). Examples of pulmonary tumor growth imaged for an empty vector-vaccinated mouse compared to the Ccl22-vaccinated mouse are shown in Fig. 6B, revealing marked differences in number and size of the tumors. Quantifying pulmonary tumors, an advantage to cutaneous Ccl22 treatment is evident (Fig. 6C). We next performed therapeutic experiments where gene gun vaccination was initiated 3 days post tumor challenge and repeated only twice before euthanasia (Fig. 6D). A remarkable reduction in tumor burden is illustrated in Fig. 6E and quantified as 39% reduction in area occupied by tumor (Fig. 6F), representing a significant therapeutic effect. We demonstrated that cutaneous Ccl22 vaccination will suppress ongoing autoimmunity accompanied by greater Treg accumulation in the skin of TCR transgenic vitiligo mouse models (19). Here, we evaluated pulmonary Treg numbers in tissues from tumor challenged mice to determine whether the same process results in reduced pulmonary immunosuppression by limiting Treg

availability. In Fig. 7A-C, images of immunostained pulmonary tissue are shown to represent $FoxP3^+$, $CD3^+$ Treg detection. A 33% greater pulmonary Treg to total T cell ratio was observed in untreated mice (Fig. 7D), with the majority of T cells expressing FoxP3 in untreated mice whereas Treg were in the minority in pulmonary tissue from Ccl22 vaccinated mice (n=3, $P<0.05$). In separate efforts to quantify $FoxP3^+$ cells immunoenzymatically we found a 2.8 fold greater pulmonary Treg density in untreated mice (n=5, $P<0.01$, not shown). Conversely, in the skin where Treg densities are generally markedly lower than in pulmonary tissues, a 45% increase in the ratio of Treg among T cells was found among tumor-bearing Ccl22-vaccinated over tumor-bearing control mice (Fig. 7E-G; n=3 $P<0.05$), indicating that Treg were redirected to the skin. A 13.9 fold increase in absolute Treg densities following Ccl22 vaccination was reported in the absence of tumor (19), yet here we calculated Treg density as a fraction of total infiltrating T cells as the more important parameter to reflect Treg function. The reduced proportion of Treg apparently resulted in reduced suppression and a 57% expansion of T cells overall as evaluated in 3 tumors/group ($P<0.01$) (Fig. 7H), whereas NK cell abundance was not significantly affected (Fig. 7I). Treatment similarly revealed a trend towards 38% increased apoptosis among tumor cells at 3 tissues/group (Fig.7J), suggesting that reduced tumor growth partially results from impaired proliferation instead. Thus cutaneous overexpression of Ccl22 can divert Treg away from tumor metastases, suggesting that equivalent treatment of human skin can be of immediate benefit to patients with melanoma metastases.

DISCUSSION

We observed overexpression of Treg chemoattractant cytokines in melanoma *in situ* tumors compared to unaffected human skin. Overexpression of CCL22 in melanoma has been associated with an accumulation of plasmacytoid DCs (23). These studies also accentuate the contribution of the tumor microenvironment to immunosuppression in melanoma. Thus, another strategy to circumvent tumor immunosuppression could be to convert immunosuppressive pDCs into a phenotype more supportive of anti-tumor immunity. Oversecretion of CCL1, meanwhile, can possibly be ascribed to infiltrating γδ-T cells and NK cells (24), which are more likely to support immune reactivity to tumors. Our studies suggest that the contribution of CCL1 to chemoattraction of Treg is not very selective. Yet the contribution of the CLA-P-selectin axis in attracting Treg may be a positive one; CLA is overexpressed by skin-infitrating T cells and favors skin over tumor homing (25).

Overexpression of chemokine receptors including CXCR3 on T cells in tumor patients and intratumoral overexpression of the associated chemokines is beneficial in the case of tumor-reactive effector cells (26, 27). Interestingly, much importance has been assigned to tumor overexpression of Ccl2, an additional ligand for CCR4 (28). Perhaps the ambivalent outcomes when promoting such interaction is due to an overarching support for Treg infiltration. We initially reported that Treg in blood from melanoma patients overexpress CCR4 (and CCR8) and may thus be preferentially *en route* to the tumor (Klarquist et al, Pigment Cell Melanoma Res 22: pp495 (abstract)). It was later shown that blocking CCR4 can prevent the immunosuppressive consequences of Treg infiltration to tumors (29). Meanwhile, we developed an interest in rerouting Treg that were sparse in vitiligo and decided to address both deficiencies at once by overexpressing CCL22. This concept is

supported by cutaneous Ccl22 overexpression suppressing vitiligo, accompanied by preferential cutaneous Treg infiltration (19). Furthermore, that outcome is supported by overexpression of CCR4 among melanoma patient Treg.

Gene gun vaccination has been applied to human subjects vaccinated against HPV (28**). One advantage of DNA vaccination is that it allows for longer lasting expression of the gene product. However, other methods of introducing CCL22 DNA may be more suitable, such as a microneedle, tattooing or electroporation (30, 31, 32). The most effective means of vaccination likely depends on the encoded gene product.

Remarkably, cutaneous overexpression of CCL22 may supersede the effects of CCL22 naturally overexpressed in the tumor. This leads us to believe that redirecting Treg may be of particular importance to the treatment of micrometastases, whereas larger tumors with greater CCL22 expression may require more drastic treatment. Redirecting Treg might also be useful in other cancers where $CCR4^+$ Treg reportedly interfere with anti-tumor responses, including colon carcinoma, lymphoma and glioblastoma (33, 34, 35). Support for our strategy is most convincing when investigating larger sample numbers, yet our materials were limited.

The proposed cutaneous overexpression of CCL22 may have consequences that can negatively impact its application in patients. We specifically investigated the possibility that exposure to CCL22 may convert T cells into Tregs, as reported for TGF-β (36), since we have proposed cutaneous overexpression as a treatment modality for vitiligo (19). The CCL22-mediated enhancement of anti-tumor responses is however not due to conversion, but rather to redirection of existing regulatory T cells to the site of cutaneous overexpression. The added benefit of suppressing autoimmunity commonly associated with anti-melanoma responses can be significant (37). Few mechanisms of supporting anti-tumor responses will simultaneously allow for reducing autoimmune side effects of therapy. Cutaneous overexpression of CCL22 may truly separate autoimmunity from anti-tumor immunity (38).

Acknowledgments

Financial support: NIH/NCI RO1CA191317 and NIH/NIAMS RO1AR057643 to I.C. Le Poole, PI and NIH/NHLBI T35HL120835 to P. Farhangi Oskuei (N.J. Zeleznik-Le Ph.D., PI).

REFERENCES

1. Fritzsching E, Kunz P, Maurer B, Pöschl J, Fritzsching B. Regulatory T cells and tolerance induction. Clin Transplant. 2009; 23S21:10–4.
2. Wang X, Dong H, Li Q, Li Y, Hong A. Thioredoxin induces Tregs to generate an immunotolerant tumor microenvironment in metastatic melanoma. Oncoimmunology. 2015; 4:e1027471. [PubMed: 26405597]
3. Schreiber TH, Wolf D, Bodero M, Podack E. Tumor antigen specific iTreg accumulate in the tumor microenvironment and suppress therapeutic vaccination. Oncoimmunology. 2012; 1:642–8. [PubMed: 22934256]
4. O'Callaghan DS, Rexhepaj E, Gately K, Coate L, Delaney D, O'Donnell DM, et al. Tumour islet Foxp3+ T-cell infiltration predicts poor outcome in non-small cell lung cancer. Eur Respir J. 2015; 46:1762–72. [PubMed: 26541534]

5. Maneechotesuwan K, Kasetsinsombat K, Wamanuttajinda V, Wongkajornsilp A, Barnes PJ. Statins enhance the effects of corticosteroids on the balance between regulatory T cells and Th17 cells. Clin Exp Allergy. 2013; 43:212–22. [PubMed: 23331562]
6. Vandenberk L, Van Gool SW. Treg infiltration in glioma: a hurdle for antiglioma immunotherapy. Immunotherapy. 2012; 4:675–8. [PubMed: 22853753]
7. Wei S, Kryczek I, Zou W. Regulatory T-cell compartmentalization and trafficking. Blood. 2006; 108:426–31. [PubMed: 16537800]
8. Zou W. Regulatory T cells, tumour immunity and immunotherapy. Nat Rev Immunol. 2006; 6:295–307. [PubMed: 16557261]
9. Nishikawa H, Sakaguchi S. Regulatory T cells in tumor immunity. Int J Cancer. 2010; 127:759–67. [PubMed: 20518016]
10. Sugiyama D, Nishikawa H, Maeda Y, Nishioka M, Tanemura A, Katayama I, et al. Anti-CCR4 mAb selectively depletes effector-type FoxP3+CD4+ regulatory T cells, evoking antitumor immune responses in humans. Proc Natl Acad Sci U S A. 2013; 110:17945–50. [PubMed: 24127572]
11. Motz GT, Santoro SP, Wang LP, Garrabrant T, Lastra RR, Hagemann IS, et al. Tumor endothelium FasL establishes a selective immune barrier promoting tolerance in tumors. Nat Med. 2014; 20:607–15. [PubMed: 24793239]
12. Nishikawa H, Sakaguchi S. Regulatory T cells in cancer immunotherapy. Curr Opin Immunol. 2014; 27:1–7. [PubMed: 24413387]
13. Ueda R. Clinical Application of Anti-CCR4 Monoclonal Antibody. Oncol. 2015; 89S1:16–21.
14. Kong YC, Jacob JB, Flynn JC, Elliott BE, Wei WZ. Autoimmune thyroiditis as an indicator of autoimmune sequelae during cancer immunotherapy. Autoimmun Rev. 2009; 9:28–33. [PubMed: 19254781]
15. Bin Dhuban K, Piccirillo CA. The immunological and genetic basis of immune dysregulation, polyendocrinopathy, enteropathy, X-linked syndrome. Curr Opin Allergy Clin Immunol. 2015; 15:525–32. [PubMed: 26485097]
16. Klarquist J, Denman CJ, Hernandez C, Wainwright DA, Strickland FM, Overbeck A, et al. Reduced skin homing by functional Treg in vitiligo. Pigment Cell Melanoma Res. 2010; 23:276–86. [PubMed: 20175879]
17. Mantovani A, Gray PA, Van Damme J, Sozzani S. Macrophage-derived chemokine (MDC). J Leukoc Biol. 2000; 68:400–4. [PubMed: 10985257]
18. Chatterjee S, Eby JM, Al-Khami AA, Soloshchenko M, Kang HK, Kaur N, et al. A quantitative increase in regulatory T cells controls development of vitiligo. J Invest Dermatol. 2014; 134:1285–94. [PubMed: 24366614]
19. Eby JM, Kang HK, Tully ST, Bindeman WE, Peiffer DS, Chatterjee S, et al. CCL22 to Activate Treg Migration and Suppress Depigmentation in Vitiligo. J Invest Dermatol. 2015; 135:1574–80. [PubMed: 25634358]
20. Schneider CA, Rasband WS, Elicieri KW. NIH Image to ImageJ: 25 years of image analysis. Nat Meth. 2012; 9:671–5.
21. Wertel I, Surówka J, Polak G, Barzyński B, Bednarek W, Bojarska-Junak A, et al. Macrophage-derived chemokine CCL22 and regulatory T cells in ovarian cancer patients. Tumour Biol. 2015; 36:4811–4817. [PubMed: 25647263]
22. Freier CP, Kuhn C, Rapp M, Endres S, Mayer D, Friese K, et al. Expression of CCL22 and infiltration by reguolatory T cells are increased in the decidua of human miscarriage placentas. Am J Reprod Immunol. 2015; 74:216–227. [PubMed: 25922986]
23. Aspord C, Leccia MT, Charles J, Plumas J. Plasmacytoid dendritic cells support melanoma progression by promoting Th2 and regulatory immunity through OX40L and ICOSL. Cancer Immunol Res. 2013; 1:402–15. [PubMed: 24778133]
24. Ebert LM, Meuter S, Moser B. Homing and function of human skin gammadelta T cells and NK cells: relevance for tumor surveillance. J Immunol. 2006; 176:4331–6. [PubMed: 16547270]
25. Clark RA, Kupper TS. IL-15 and dermal fibroblasts induce proliferation of natural regulatory T cells isolated from human skin. Blood. 2007; 109:194–202. [PubMed: 16968902]

26. Clancy-Thompson E, Perekslis TJ, Croteau W, Alexander MP, Chabanet TB, Turk MJ, et al. Melanoma induces, and adenosine suppresses, CXCR3-cognate chemokine production and T–cell infiltration of lungs bearing metastatic-like disease. Cancer Immunol Res. 2015; 3:956–67. [PubMed: 26048575]
27. Dengel LT, Norrod AG, Gragory BL, Clancy-Thompson E, Burdick MD, Strieter RM, et al. Interferons induce CXCR3-cognate chemokine production by human metastatic melanoma. J Immunother. 2010; 33:965–74. [PubMed: 20948440]
28. Zhang T, Somasundaram R, Berencsi K, Caputo L, Gimotty P, Rani P, et al. Migration of cytotoxic T lymphocytes toward melanoma cells in three-dimensional organotypic culture is dependent on CCL2 and CCR4. Eur J Immunol. 2006; 36:457–67. [PubMed: 16421945]
29. Chang DK, Peterson E, Sun J, Goudie C, Drapkin RI, Liu JF, et al. Anti-CCR4 monoclonal antibody enhances antitumor immunity by modulating tumor-infiltrating Tregs in an ovarian cancer xenograft humanized mouse model. Oncoimmunol. 2015; 2(3):e1090075.
30. Trimble C, Lin CT, Hung CF, Pai S, Juang J, He L, et al. Comparison of the CD8+ T cell responses and antitumor effects generated by DNA vaccine administered through gene gun, biojector, and syringe. Vaccine. 2003; 21:4036–42. [PubMed: 12922140]
31. McCaffrey J, Donnelly RF, McCarthy HO. Microneedles: an innovative platform for gene delivery. Drug Deliv Transl Res. 2015; 5:424–37. [PubMed: 26122168]
32. DeMuth PC, Min Y, Huang B, Kramer JA, Miller AD, Barouch DH, et al. Polymer multilayer tattooing for enhanced DNA vaccination. Nat Mater. 2013; 12:367–76. [PubMed: 23353628]
33. Svensson H, Oloffson V, Lundin S, Yakkala C, Björck S, Börjesson L, et al. FoxP3+CD25(hi) regulatory T cells in colon adenocarcinomas correlate to reduced activation of conventional T cells. PLoS One. 2012; 7(2):e30695. [PubMed: 22319577]
34. Ishida T, Ueda R. Immunopathogenesis of lymphoma: focus on CCR4. Cancer Sci. 2011; 102:44–50. [PubMed: 21044233]
35. Jacobs JF, Idema AJ, Bol KF, Grotenhuis JA, de Vries IJ, Wesseling P, et al. Prognostic significance and mechanism of Treg infiltration in human brain tumors. J Neuroimmunol. 2010; 225:195–9. [PubMed: 20537408]
36. Khattar M, Chen W, Stepkowski SM. Expanding and converting regulatory T cells: a horizon for immunotherapy. Arch Immunol Ther Exp (Warsz). 2009; 57:199–204. [PubMed: 19479206]
37. Byrne KT, Turk MJ. New perspectives on the role of vitiligo in immune responses to melanoma. Oncotarget. 2011; 2:684–94. [PubMed: 21911918]
38. Kimpfler S, Sevko A, Ring S, Falk C, Osen W, Frank K, et al. Skin melanoma development in ret transgenic mice despite the depletion of CD25+Foxp3+ regulatory T cells in lymphoid organs. J Immunol. 2009; 183:6330–7. [PubMed: 19841169]

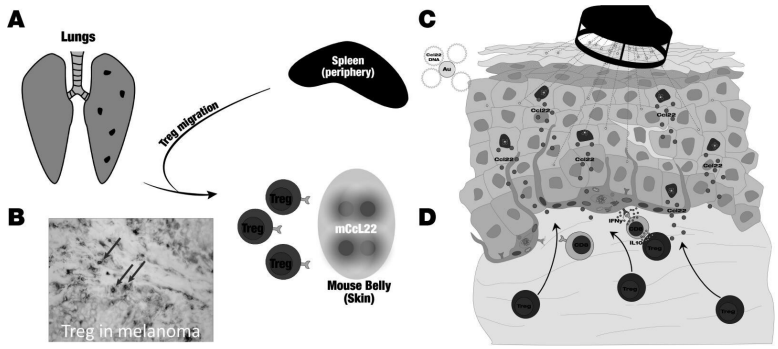

Fig. 1. Study concept: CCL22 to divert Treg and support anti-tumor responses in melanoma

(A) Melanoma cells commonly metastasize to the lung, generating surface lesions detectable as pigmented spots. (B) In human melanoma, Treg are detectable by nuclear FoxP3 expression (red) and membrane CD3 staining (blue) resulting in double stained cells (purple arrows) that can be enumerated as a fraction of total T cells (C) Vaccination using plasmid DNA encoding Ccl22 is applied to ventral murine skin to provide proof of concept for (D) diverting Treg away from the circulation and towards skin.

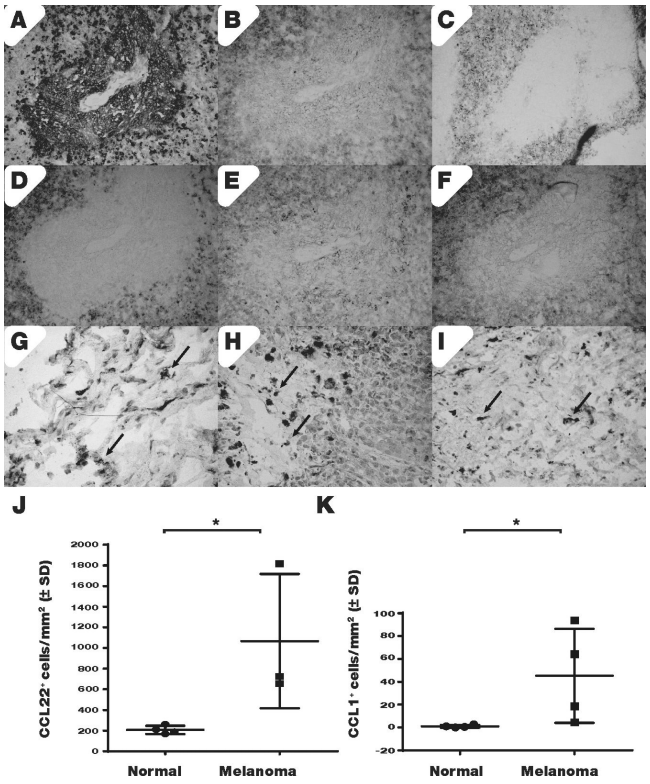

Fig. 2. Treg chemoattractant cytokines are abundant in melanoma tumors

(A) Expression of melanoma marker TRP-1 in a spinal metastasis is inversely related to (B) FoxP3 expression detected just outside a melanoma lesion whereas (C) such FoxP3 expression colocalizes with CCR4 chemokine receptor expression and (D) faint CCL22 expression detected in the same area. (E) CCR8 chemokine receptor expression and TRP-1 expression are likewise readily mutually exclusive whereas (F) CCL1 expression again colocalizes with its receptor CCR8 in areas surrounding the metastasis. In metastatic lesions of the (G) lung, (H) lymph node and (I) brain, similar distributions of CCL22-expressing cells are observed. Under (J) we quantified CCL22 expression in 3 melanoma *in situ* samples compared to 4 unaffected adult skin samples, detecting 5-fold upregulated chemokine expression whereas (K) an 8-fold upregulation of CCL1 expression was observed.

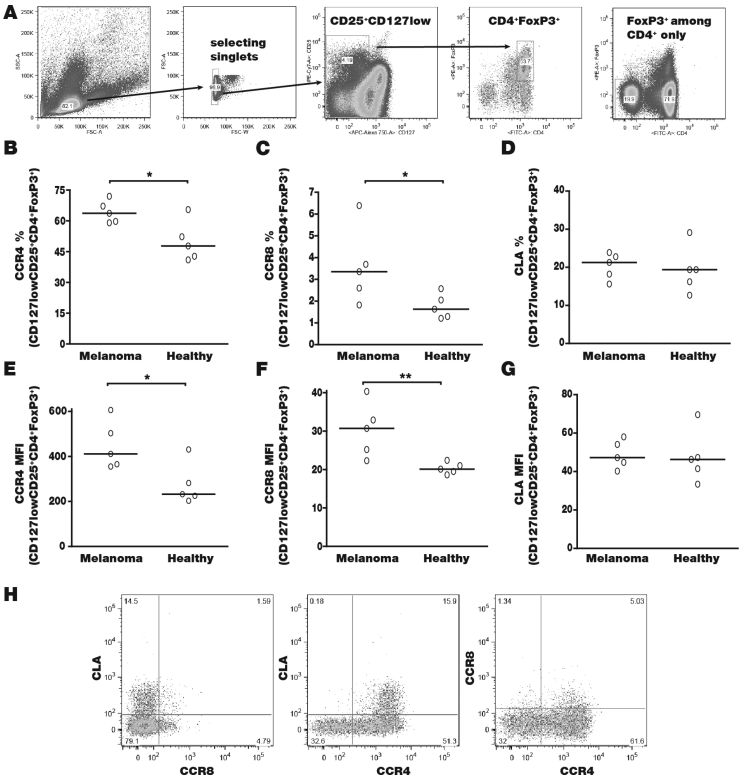

Fig. 3. Circulating Treg from melanoma patients overexpress chemokine receptors

(A) Treg were selected based on forward/side scatter and singlet selection, as $CD25^{+}CD127^{low}$, FoxP3-expressing $CD4^{+}$ cells. For comparison, selection of $FoxP3^{+}$ cells among $CD4^{+}$ cells is shown without including $CD127^{low}$. The percentage of (B) $CCR4^{+}$, (C) $CCR8^{+}$ and (D) CLA^{+} Tregs are compared between 5 melanoma patients and 5 healthy controls, indicating a significant increase in the number of CCR4 and CCR8 expressing Tregs ($P<0.05$ for each). When examining mean fluorescence intensities for (E) CCR4 expression, (F) CCR8 expression and (G) CLA, these receptors are upregulated as well ($P<0.05$ for CCR4 and <0.01 for CCR8). In (H) it is clear that the population overexpressing CCR4 also incorporates most CLA expressing, and the majority of CCR8 expressing Tregs.

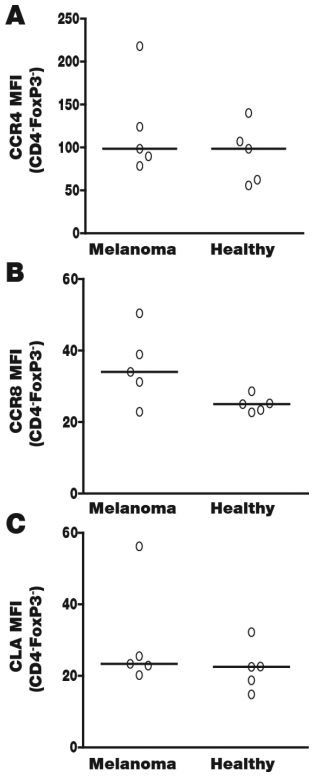

Fig. 4. CCR4 is not elevated on the surface of circulating CTL

If Treg were to be rerouted based on chemokine receptor expression, selective upregulation on the Treg subset is critical. Thus we probed $CD4^{-}$, $FoxP3^{-}$ T cells for preferential expression of (A) CCR4, noting similar expression among healthy and melanoma non-regulatory T cells that is less than half of what is observed on Tregs (see Fig. 3). (B) CCR8 expression does not differ significantly between 5 patients and 5 controls, whereas MFIs are not reduced compared to Tregs. (C) CLA expression (MFI) is also the same among patients and controls. Overall however, expression is markedly (65%) higher among Treg ($P<0.05$). Though Treg may be selectively targetable via CLA, the number of CCR4 expressing patient Treg is markedly greater.

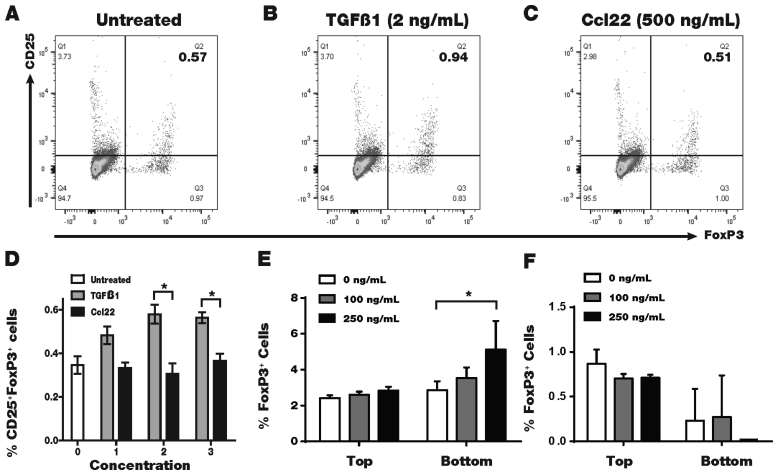

Fig. 5. CCL22 favors Treg migration but does not convert T cells to become Treg

To demonstrate that Ccl22 vaccination increases the fraction of skin Treg without converting T cells into Treg, we exposed 3 samples of T cells from a FoxP3 reporter mouse to Ccl22 or to TGF-β overnight. Splenocytes were gated for $CD3^+$ T cells and exposed to CD4 and CD25 immunostaining. (A) $FoxP3^+CD25^+$ Treg in a representative untreated sample, (B) Treg abundance is increased in a representative sample of TGFβ treated cells whereas (C) exposure to Ccl22 does not induce a Treg phenotype *in vitro*. (D) Tregs are quantified, demonstrating a significant increase in response to 2 and 20 ng/mL TGF-β of up to 60%. (E) In a representative transwell migration assay among 3 performed, Treg abundance is increased among splenocytes migrating towards Ccl22, whereas (F) preferential Treg migration is not observed towards Ccl1.

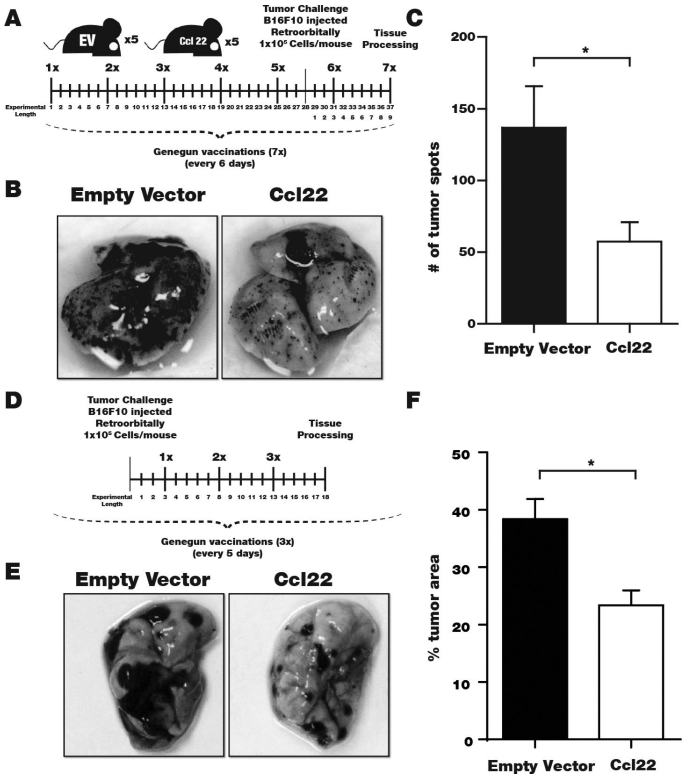

Fig. 6. Tumor growth is inhibited by cutaneous Ccl22 overexpression

(A) In a representative experiment of 2 performed, 5 mice/group were gene gun vaccinated with Ccl22-encoding or empty vector DNA as shown. (B) At euthanasia, lung tissues were collected to identify tumors (C) Significantly reduced pulmonary tumor counts were observed in Ccl22 vaccinated mice as quantified for 5 mice/group ($P<0.05$). (D) In therapeutic experiments, mice were tumor challenged 3 days before vaccination applied every 5 days as shown (E) Examples of pulmonary tissues from the Ccl22 (n=7) and empty vector control (n=8) groups. (F) Trimmed means (highest and lowest values removed from each group) were used to calculate that significantly reduced portions of the lung surface were covered by tumor in Ccl22 mice (representative experiment of 2 performed).

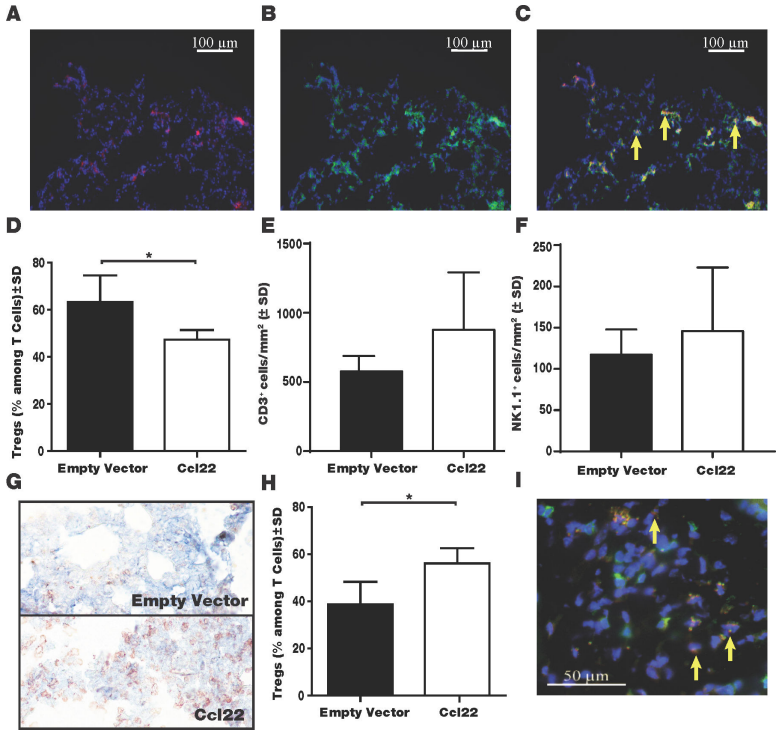

Fig. 7. Cutaneous Ccl22 overexpression limits tumor infiltrating Treg

Treg in formalin-fixed cryosections by immunofluorescent double staining. CD3 shown in green and FoxP3 staining in red. DAPI counterstaining was used. Shown is a sequence representing (A) FoxP3 stained and (B) CD3 stained lung tissue as well as (C) an overlay, in an untreated mouse, including DAPI counterstaining and (D) the number of Treg was quantified as a ratio to total infiltrating T cells in pulmonary tissue, revealing a marked reduction in Ccl22 vaccinated mice (n=3, *P<0.05), representative experiment of 2 evaluated. The overall abundance of pulmonary (E) T cells and (F) NK cells was not affected. (G) Example TUNEL stainings of lung tissue from empty vector (top) and Ccl22 (bottom) treated mice in a prophylactic experiment. (H) The number of Treg is elevated in the skin of vaccinated mice. (I) Tregs in a sample of Ccl22 vaccinated skin.